Downloaded from http://qjegh.lyellcollection.org/ at Massachusetts Institute of Technology on September 15, 2019

Q. J. eng. Geol. London, 1983 Vol. 16, pp. 127–134. Printed in Northern Ireland

The engineering behaviour of jointed rock mass models composed of weak and strong strata

W. R. A. Knox & M. Zacas

Department of Civil Engineering, Paisley College of Technology, High Street, Paisley, Renfrewshire PA1 2BE

Summary

The influence of the occurrence of weaker strata in a layered, jointed, model rock mass was examined. The model materials used were lightweight concrete and gypsum mortars. The models were constructed from blocks of these materials in a plane frame testing rig. The load/settlement characteristics, bearing capacity, pattern of deformation and modes of failure under a steel plate were observed, and the experimental results were then compared with those predicted by finite element analyses. No obvious correlation of results between the mathematical models and the laboratory models was discovered.

Introduction

The *in situ* engineering behaviour of a rock mass varies considerably throughout the mass and is influenced by many phenomena. These can include such basic factors as the nature of the rock material itself, its micro-fabric and the macro-fabric of its discontinuities, the action of water on the rock substance and in its fabric, the stress or loading conditions imposed by engineering works, and the variation with time in fundamental properties such as mechanical strength. None of these factors is mutually exclusive, so engineering design in rock masses can be an extremely complex operation.

In particular, one significant feature of a rock mass often encountered is that of a layered or bedded structure, with the individual layers having quite different engineering properties. Such a structure can be comprised of layers of either 'strong' or 'weak' material in either complete or partial contact, with or without an infilling material between the layers. Furthermore, the layered structure can be intersected by a set or sets of joints, which can be mutually perpendicular, so a 'blocky' system exists. This can present numerous difficulties to an engineer who is faced with construction or excavation in such material.

The most basic engineering aspect of any material is its response to stress. For homogeneous, isotropic materials with predictable properties, design is generally straightforward; however, the situation facing designers in rock mechanics who must often cope with multi-layered, blocky rock masses is an extremely complex one. Many studies have been made of the problem using physical and mathematical models. Krsmanovic & Milic (1964), Trollope (1968), Hayashi (1966), Maury (1970), Maury & Habib (1970), Gasiev & Ehrlikhman (1971), Burman (1971), Chappell (1974) and Hammet (1974) are among many investigators in the field. To date, most of the work has concentrated on multi-layered systems where each layer had similar engineering characteristics. However, work by Clarke *et al.* (1970), Peck (1976) and Avramova-Tacheva & Manev (1977) has shown that the behaviour of a layered rock mass can be significantly affected by the occurrence of weaker layers with linear or non-linear characteristics.

This paper presents an investigation of the behaviour of a horizontally layered, jointed, rock model where the layers have differing engineering properties. The loading was applied to the layered model on its surface in a direction normal to the layering, in order to evaluate the influence of such parameters as the thickness of the weaker layers, their depth below the surface loading and their mechanical properties on the load-deformation characteristics of the whole structure.

Experimental programme

Model materials

Stimpson (1970) has documented the use of different materials and combination of materials used by several investigators in modelling a variety of situations in rock mechanics, as well as in other fields. His classification covers a wide range of materials, but the most commonly used one for simulating rock is gypsum, either simply as a plaster when mixed with water or as a mortar when a filler has been added. Of the mortar type, the use of Kieselgur (a diatomaceous earth, marketed under the trade name 'Cellite') as the filler has been found to produce an extremely suitable modelling material for representing what could be termed as 'low strength' rocks.

For the modelling of a 'strong' rock, Reik & Zacas (1978) successfully used a lightweight concrete. It exhibited brittle behaviour, was cheap, and easily handled and cut into model specimens.

0481-2085/83/0400-0127$02.00 © 1983 The Geological Society

Downloaded from http://qjegh.lyellcollection.org/ at Massachusetts Institute of Technology on September 15, 2019

TABLE 1.

Model material	*Uniaxial tests*				*Triaxial tests*	
	Compressive strength N/mm^2	*Tensile strength* N/mm^2	*Young's modulus* N/mm^2	*Poisson's ratio*	*Cohesion* N/mm^2	*Angle of internal friction* ϕ
Siporex lightweight concrete	6.1	1.40	1810	0.1	1.60	39.5°
Gypsum mortar SI	3.13	0.51	300	0.2	0.76	36.0°
Gypsum mortar S2	0.49	0.08	120	0.2	0.16	33.0°

In this investigation, therefore, the model materials selected to represent the 'weak' and 'strong' layers of the bedded mass were respectively:

(a) Gypsum-Kieselgur-Water mortars with proportions by weight of (i) 1:0.19:1, for a mixture designated SI, (ii) 1:0.67:2, for a mixture designated S2.

(b) A proprietary lightweight concrete manufactured by Siporex Ltd., Motherwell, Scotland.

The complete characteristics of these model materials are detailed by Zacas (1979), but Table 1 indicates their major engineering properties. The terminology of 'cohesion' and angle of 'internal friction' within the context of the triaxial test is universally accepted, but the actual meaning of these terms when applied to rock or rock modelling material is more difficult to conceive. However, the authors have conformed with tradition in interpreting the failure envelope. It may be of interest to note that the failure envelopes for all the model materials were much closer to that of the Griffith form than to the modified Griffith and Navier-Coulomb.

The actual models for testing were built up from blocks of the model material, measuring either 75 × 75 × 150 mm long, or 75 × 50 × 150 mm long. These were cut by masonry saw from slabs of the material to make a finished model of dimensions 1170 mm deep × 1170 mm wide × 150 mm long. The construction allowed the formation in the 1170 × 1170 plane of orthogonal joint sets having values for the degree of joint separation of 0.5 and 1.0, (as defined by Muller 1965) in the vertical and horizontal planes respectively.

Test arrangements

The loading system shown in Fig. 1 was used to conduct the tests. The apparatus consisted of:

(i) a rigid frame composed of steel channels, bolted together to accommodate the model and to support the hydraulic jack loading devices;

(ii) the loading system of hydraulic jacks, two of 50 kN capacity and one of 300 kN capacity; the loads were applied to the model through steel plates;

(iii) an instrumentation system which was used to measure loads and displacements; the loads were indicated by instrumented load cells, while surface settlements were indicated on mechanical clock gauges and displacements on the face of the model were determined using a photogrammetric technique;

(iv) a reference frame, surrounding the main support frame, comprising a 50 mm square box section steel tubing to serve as a standard frame for the photogrammetric method.

To evaluate the influence of the various parameters mentioned earlier, three series of tests were performed, simply identified as AO, AA and AB. Series AO contained just one of the model materials on its own, *viz.* that of the lightweight concrete. Series AA and AB included the same number and type of tests but using materials S1 and S2 respectively.

The actual test procedure was standardized as follows. The model was loaded using all three jacks up to an initial stress of 0.05 N/mm^2 and then slowly unloaded. This had the effect of causing an initial compaction of the model and so reduced the effect of joint misfit. The main loading was then applied through the single heavy capacity hydraulic jack on the surface of the model through the steel bearing plate of breadth B = 100 mm at a stressing rate of 0.0133 N/mm^2 min. During the loading cycle the specimen was closely and continuously observed to record the opening and/or closing of joints and the onset and progression of cracking. Photographs were taken at frequent intervals to provide a permanent record of these features.

Table 2 summarizes the test results and should be considered in conjunction with Fig. 2, where T_i is the thickness of the 'weak' stratum, Z_i is the depth to the surface of the 'weak' stratum, g_i is the number of sub-strata in the weak stratum and n is the number of weak strata in the model. The terms q and q_f require to be distinguished: q is the bearing capacity (i.e. applied stress intensity) at which considerable damage to the model had been achieved. It is the stress intensity at which the load/settlement curve starts to flatten out, and could be considered somewhat analogous to the 'Limit of Proportionality' on the stress/strain curve

Downloaded from http://qjegh.lyellcollection.org/ at Massachusetts Institute of Technology on September 15, 2019

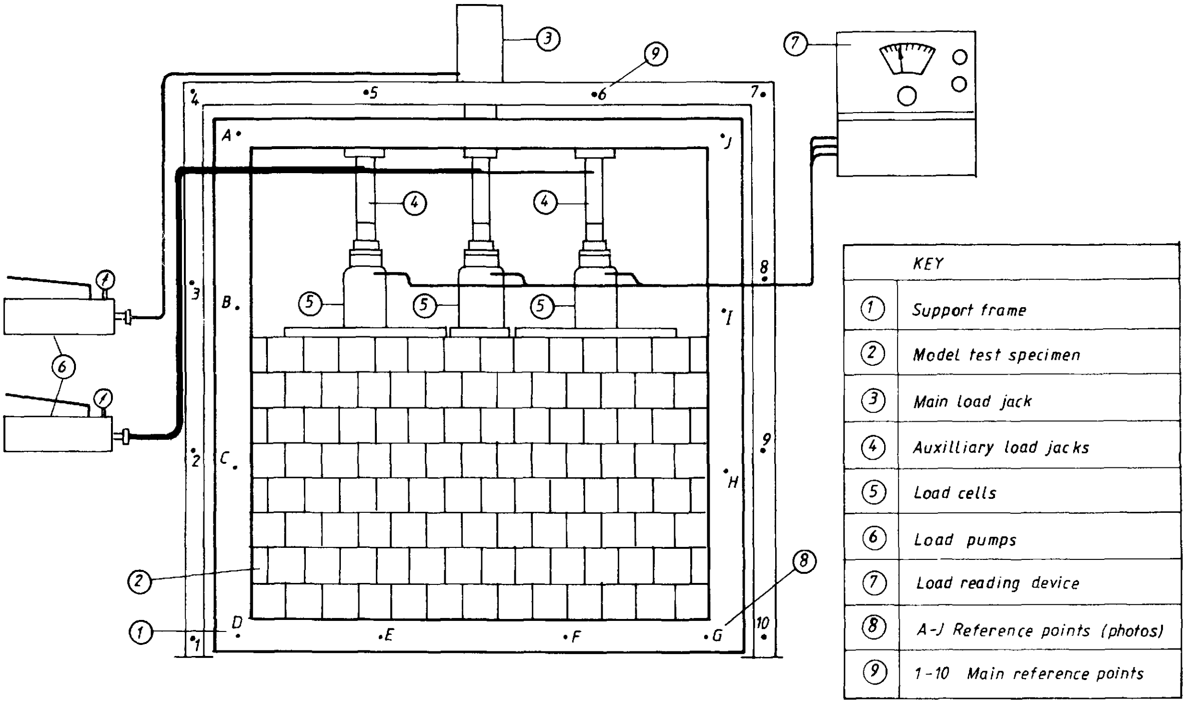

FIG. 1. Loading and monitoring facilities used for the experiments.

TABLE 2. *Test characteristics, bearing capacity and ultimate bearing capacity of the specimens*

Test no.	*Model material* *Strong*	*Weak*	*No. of weak strata* n	*No. of sub-strata* g_i	*Thickness of weak stratum* T_i (mm)	*Depth to surface of weak stratum* Z_i (mm)	*Bearing capacity at yield* q	*Ultimate bearing capacity* q_f	*Bearing capacity ratio* q/q_f
A0	LC	—	—	—	—	—	4.25	4.66	0.91
AA1	LC	SI	1	1	50	0	2.25	2.60	0.87
AA2	LC	SI	1	1	50	75	2.75	3.05	0.90
AA3	LC	SI	1	1	50	150	3.00	3.40	0.88
AA4	LC	SI	1	1	50	225	3.20	3.65	0.88
AA5	LC	SI	1	3	150	0	1.95	2.20	0.89
AA6	LC	SI	1	3	150	150	2.80	3.25	0.86
AA7	LC	SI	3	1	50	75/200/325	2.50	2.85	0.88
AB1	LC	S3	1	1	50	0	0.51	0.62	0.82
AB2	LC	S3	1	1	50	75	0.68	0.80	0.85
AB3	LC	S3	1	1	50	150	0.90	1.01	0.89
AB4	LC	S3	1	1	50	225	1.02	1.20	0.85
AB5	LC	S3	1	3	150	0	0.39	0.45	0.89
AB6	LC	S3	1	3	150	150	0.78	0.92	0.85
AB7	LC	S3	3	1	50	75/200/325	0.60	0.73	0.82

Downloaded from http://qjegh.lyellcollection.org/ at Massachusetts Institute of Technology on September 15, 2019

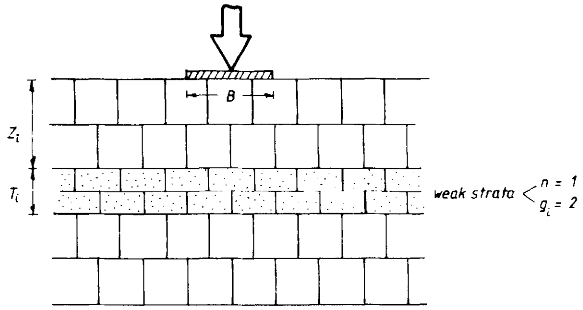

FIG. 2. Strata nomenclature.

for a steel, for example. q_f is the ultimate bearing capacity and represents the stress intensity at complete rupture of the model.

Model test results

In each test, the load/surface settlement (or stress/strain) behaviour, the pattern of deformation, the bearing capacity and the mode of failure were observed.

The load/settlement curves for the AA and AB series of tests are shown in Figs 3 and 4 respectively, with the axes shown in both the forms of P (load) against δ (settlement), and stress σ ($=P/A$, where A is the area of the loaded plate) against strain ε ($=\delta/B$, where B is the plate width). These curves then give rise to the parameters E_{DC}, (the 'specific modulus of deformation'), E_{SC}, (the 'specific secant modulus') and E_{TC} (the 'specific tangent modulus'). These provide a basis from which behavioural characteristics of the model can be assessed. They are obtained from the curves by the methods based on the Boussinesq solution for the normal displacement of the surface of a semi-infinite elastic solid under the action of a point load.

Also included in Figs 3 and 4, for comparison, is the load/settlement curve for model AO, (i.e. the one composed entirely of lightweight concrete, with no weaker strata at all). The most obvious facts emerging from these graphs are that: (i) the inclusion of a weak stratum anywhere reduced the overall bearing capacity and increased the deformability of the model; and (ii) the nearer to the surface that the weak stratum was located the worse was the effect on these two parameters. This was to be expected on any logical basis, but it is reassuring that the figures now proved it to be so.

Figure 5 shows the relationship between deformability and location of the weak stratum. The deformability is expressed as a tangent modulus ratio E_{TC}/E'_{TC} where E_{TC} is the tangent modulus of the model containing weak strata and E'_{TC} is the tangent modulus of the model with no weak strata.

Curves 1A and 1B in Fig. 5 apply to the model where the weak strata were composed of model material S1, while curves 2A and 2B refer to the model with S2 as the material in the weak strata. Again, it is apparent that the overall deformability of the model is more strongly influenced simply by the presence of a weaker stratum than by its actual thickness. It is clear that the deformability of the model with weak strata composed of S2 material was almost

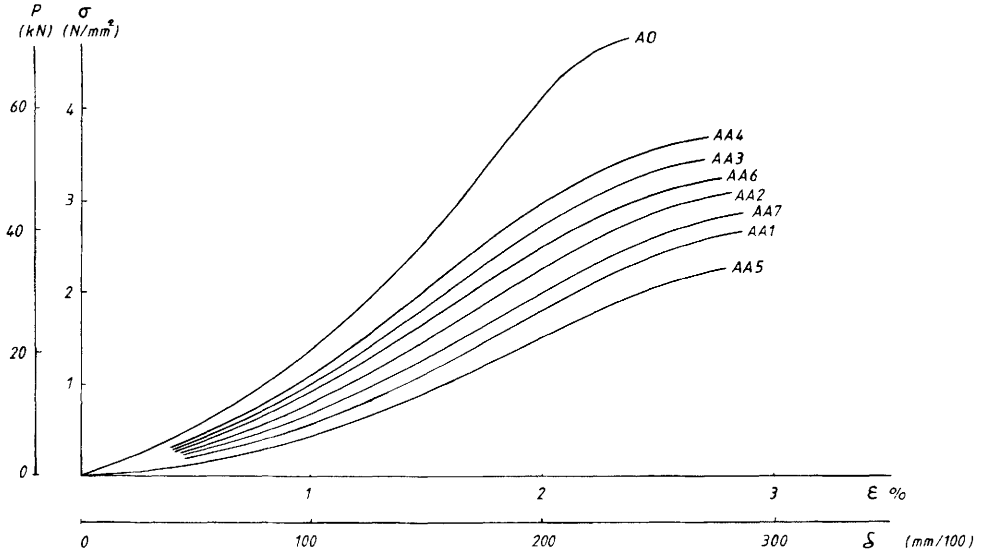

FIG. 3. Load-settlement, stress–strain curves for AA series of tests.

Downloaded from http://qjegh.lyellcollection.org/ at Massachusetts Institute of Technology on September 15, 2019

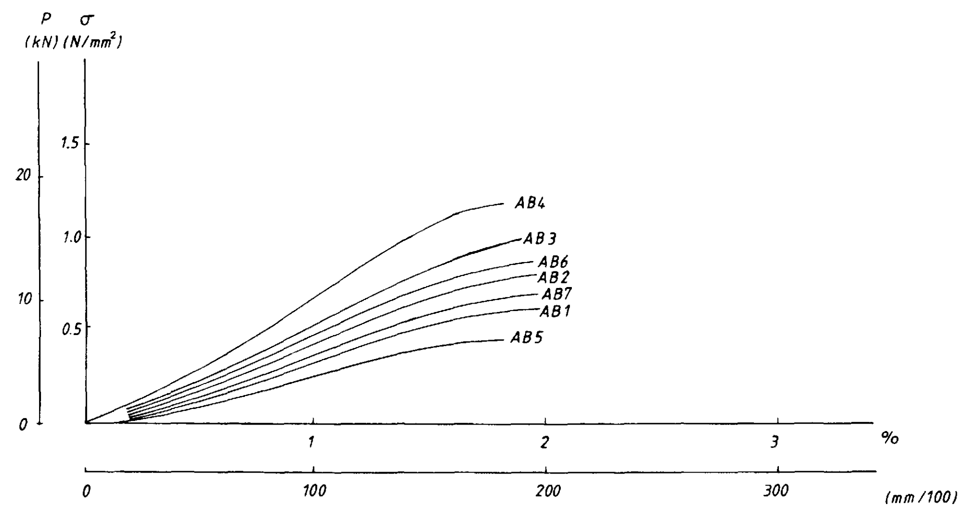

FIG. 4. Load-settlement, stress–strain curves for AB series of tests.

three times that of the corresponding model with S1 as its weak strata. The ratio of the modulus of elasticity of S1 material to S2 material was 2.5:1, so there appears to be a link between the deformability of the mass and the deformability of the components, any difference being possibly due to unavoidable small differences in the actual construction of the models.

With regard to vertical deformations directly beneath the loaded area, it is to be seen from Fig. 6 that they varied inversely with depth from the loaded area

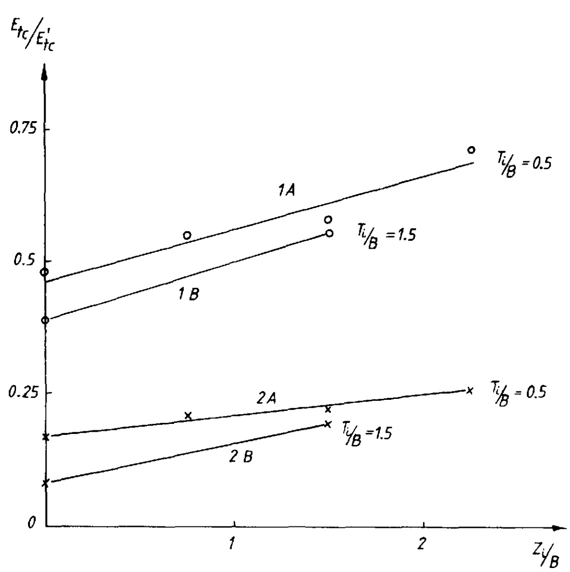

FIG. 5. Relative deformability–depth of weak strata relationship (1A,1B: Material S1 for weak strata; 2A,2B: Material S2 for weak strata). For notation see Fig. 2.

(which was to be expected), diminishing rapidly at depths greater than a distance equal to 2B. The practical values measured here did not, however, provide any general relationship between failure displacements and the depth or thickness of the weak strata. Nevertheless, several points emerge from looking at the observed in-plane displacements. Firstly, they are concentrated at the level of the weak stratum, i.e. the vertical deformations below the weak stratum were just 30–40% of that above it. In other words, the weak stratum was acting as a 'damping' agent with respect to the vertical movement. When horizontal displacements are considered, the maximum amounted to 17% of the maximum vertical displacement when S1 was the weak stratum, and 31% for the same ratio when S2 was the weak stratum. This has a bearing on the rotational stability of the jointed blocks immediately above the weak stratum.

The next point for discussion is that of the so-called 'bearing capacity' of the models. Perhaps this is the most significant parameter from a practical engineering point of view, because the problem facing any designer who wishes to establish a foundation on rock is the decision as to what load the rock mass can sustain. It would be extremely useful to quantify the bearing capacity of a layered rock mass in terms of strength parameters of the individual strata in the mass, and to this end Fig. 7 was established. When ρ and λ are defined as shown:

$$\rho = \frac{q}{q_{us}}$$

where q = bearing capacity of model and q_{us} = unconfined compressive strength of the strong model material (i.e. Siporex) and

$$\lambda = \frac{q_{uw}}{q_{us}}$$

Downloaded from http://qjegh.lyellcollection.org/ at Massachusetts Institute of Technology on September 15, 2019

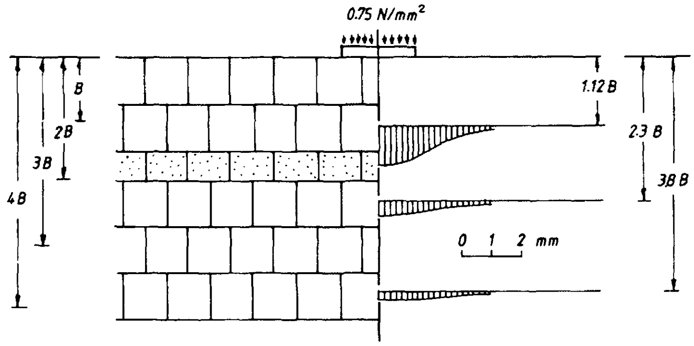

FIG. 6. Typical test deformations (Test AB3).

where q_{uw} = unconfined compressive strength of the weak model material then Fig. 7 indicates that the bearing capacity of the model would appear to lie between certain limits, these limits being governed by the individual uniaxial compressive strengths of the model materials and the position of the weak strata in the model. This is logical, but it has now been quantified. A hatched area is shown in which the bearing capacity of the model could be placed, the limits of the area depending on the relative locations of the weak strata. It is tempting then to consider that a range of bearing capacities of any model structure could be predicted from Fig. 7, knowing the uniaxial compression strengths of the individual model materials.

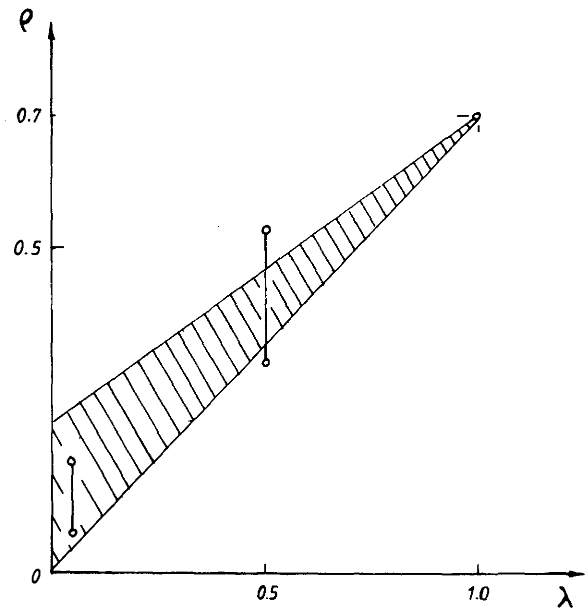

FIG. 7. Bearing capacity ratio (ρ)–uniaxial strength ratio (λ) relationship. For definitions see text.

To complete the bearing capacity study, Fig. 8 has been included to show that the depth of the weak stratum within the model has a significant influence on the bearing capacity, as stated above. The actual strength of the weak stratum is of greater significance than either its location or thickness, but the effect of these two latter factors is also obvious.

Not only is bearing capacity of rock important, but so is the deformability of the material *en masse*. Figure 9 is an attempt to quantify the deformation characteristics of the model. When ξ is defined as shown,

$$\xi = E_w/E_s$$

where E_w = Young's Modulus of Elasticity of the weak material and E_s = Young's Modulus of Elasticity of the strong material, then a linear fit between ρ and ε was not found to exist and a log plot was adopted.

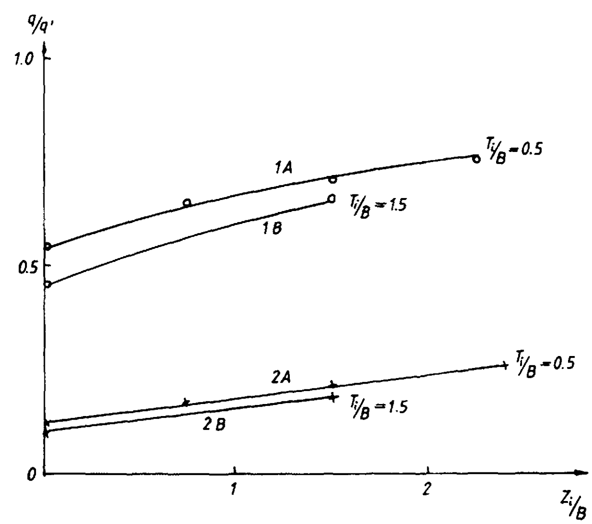

FIG. 8. Relative bearing capacity–depth of weak strata relationship (notation as in Fig. 5).

Downloaded from http://qjegh.lyellcollection.org/ at Massachusetts Institute of Technology on September 15, 2019

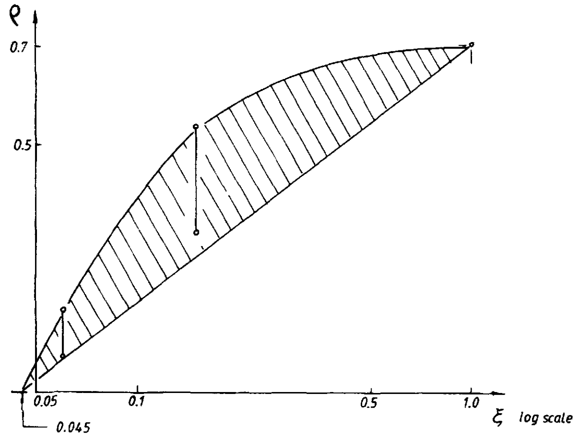

FIG. 9. Bearing capacity ratio (ρ)–modulus of elasticity ratio (ε) relationship.

TABLE 3. *Joint properties*

Model material of joint walls	*Normal stiffness* K_n(N/mm^2)	*Shear stiffness* K_s(N/mm^3)	*Angle of friction* j	*Max. joint closure* V_m(mm)
LC–LC	9.0*	1.0	39.5°	0.078
SL–S1	40.0*	0.8	36.0°	0.035
S3–S3	60.0*	0.5	34.0°	0.028
LC–S1	20.0†	0.85	36.0°	0.050†
LC–S3	30.0†	0.55	36.0°	0.030†

* Average values up to σ_n = 3.0 N/mm^2.
† Assumed values.

Even this plot is not promising but, for the number of full scale tests which were carried out, there would appear to be limits between which the deformability of the model could lie. The obvious reason for the lack of a better fit with the deformation data is that there probably existed different degrees of joint misfit among the models tested. This would have a bigger influence on deformation than on bearing capacity.

With regard to modes of failure, various types were apparent. All failures were progressive; joint separation started at stressing levels as low as $0.15q$ and cracking in intact blocks was observed at $0.2q$, where q is the bearing capacity of the model as defined previously. This is yet further evidence that, in the 'compressive' failure of brittle materials, the mechanism is one of crack propagation, whether by tension or shear, commencing at relatively low stress levels. A figure of 20% ultimate uniaxial compressive strength is typical for concrete (Knox 1967). Three types of failure mechanisms can be identified:
(a) a punching shear, occasionally combined with a bending action of the weak stratum;
(b) a 'wedge' type joint opening between blocks in the strong strata combined with a sinking of these blocks into the weak stratum, resulting in a punching shear fracture in it; and
(c) a 'wedge' type joint opening between blocks in the strong strata combined with fracturing of the weak blocks.
No one particular failure mode seemed to dominate.

Numerical analysis

There are numerous 'elastic' solutions for special cases of stresses and displacements in layered rock or rock systems, and Poulos & Davis (1974) summarize the large amount of curves charts and tables available for such cases. Unfortunately, nature does not always oblige by giving the engineer 'elastic' soils and rocks. However, recent attempts using the Finite Element Method (FEM), for example Zienkiewicz (1979), have shown that this procedure can be used to solve stress and deformation problems in multi-layered systems.

It was decided to compare the experimental deformation values measured in the laboratory model with those which were provided by the Finite Element approach. In adopting the 'implicit joint analysis' finite element program (Duncan & Goodman 1968), modifications were made to take account of cases where the degree of joint separation was not equal to unity, and Table 3 shows the joint properties considered valid. Even so, the theoretical deformations differed considerably from the experimental values in this study. Typically, the theoretical displacements below a weak stratum were 0.4 to 0.8 of the corresponding ones on top of the stratum, while experimentally, the corresponding values were lower at 0.3 to 0.4. Block misfit during construction, and the inability of the program to accommodate non-linear joint behaviour could account for the discrepancies.

In addition, the use of an elasto-plastic explicit joint analysis similar to that suggested by Goodman (1976), and of Zienkiewicz's (1979) initial stress method lead to high non-linearity and divergency. In other words, even sophisticated numerical methods did not provide solutions to the value of displacements which were compatible with the observed values, and it is doubtful if any further refinements to the finite element methods used could improve the disparity.

Conclusions

The behaviour of a layered rock mass with weak and strong strata is strongly influenced by the relative engineering properties of the two materials comprising the strata. In particular, the deformability of a model jointed rock mass with weak and strong strata varied inversely with the depth of the weak stratum from the

Downloaded from http://qjegh.lyellcollection.org/ at Massachusetts Institute of Technology on September 15, 2019

loaded surface when plane stress conditions were imposed. The deformability also depended on the relative values of the modulus of elasticity of the materials, and the joint characteristics. The weak stratum, in fact, acted as a 'damping agent' for vertical deformations.

With respect to stress, the nature of the load/deformation curve, indicating an initial 'deformation-stiffening', could lead to the conclusion that there was an increase in bearing capacity, but this was not necessarily the case. The bearing capacity of the model, in fact, depended upon the comparative uniaxial compressive strength of the materials. As has been indicated in Fig. 7, it is tempting to put limiting values on the bearing capacity of the model knowing the uniaxial compressive strength ratio of the model materials. Although tentative, because of the limited number of tests conducted, this conclusion could prove to be a guide in actual design.

The finite element programs used to model the system numerically provided poor correlation with the observed behaviour. This was not unexpected: reference can be made to Naylor & Pande (1981) to see the difficulties encountered in several case studies where the numerical models required major modification to correlate with measured deformations. This is not to detract from the usefulness of the finite element method; it is a sophisticated analysis which can help in establishing how a structure, whether it be a model or a prototype, is likely to behave. It is extremely difficult, however, to derive a numerical model which will represent in every aspect the real behaviour of an engineering structure, model or otherwise.

The study was one on model behaviour and was also a plane stress problem. Model studies in isolation from real field observations are always unrealistic and their use in design without *in situ* confirmation is certainly not advised. However, the practical problems associated with the observation of the real engineering behaviour of actual jointed rock masses with weak and strong strata have limited the amount of work carried out in this field; laboratory model studies can help in such difficult cases.

The plane stress situation in the model study may not be entirely realistic in geotechnical design; however, the underlying philosophy was to establish the behaviour of the model under known boundary conditions and compare this with numerical predictions with the same boundary conditions.

References

AVRAMOVA-TACHEVA, E. & MANEY, G. (1977). Kinds of Structurally Complex Formations and an Approach for Valuation of their Mechanical Behaviour, Proc. Symp. Geotech. Structurally Complex Formations, **1,** 19–27.

BURMAN, B. C. (1971). *A Numerical Approach to the Mechanics of Discontinua.* Thesis, PhD James Cook University.

CHAPPELL, B. A. 1974. Numerical and Physical Experiments with Discontinua. *Proc. of 3rd Congress of ISRM* **2A,** 118–25.

CLARKE, C. L., *et al* 1970. Foundation Conditions at Muda Dam. *Proc. of 2nd Congress of ISRM* **3,** 6–15.

DUNCAN, J. M. & GOODMAN, R. E. 1968. *Finite Element Analyses of Slopes in Jointed Rock.* U.S. Army Eng. Waterways Experimental Station, Vicksburg, Contract No. DAC-W39-67-C-0091.

GASIEV, E. G. & ERLIKHMAN, S. A. 1971. Stresses and Strains in Anisotropic Rock Foundations. *International Symposium on Rock Mechanics.* Nancy Report 11–1.

GOODMAN, R. E. 1976. *Methods of Geological Engineering in Discontinuous Rocks.* West Publishing Co., New York.

HAMMETT, R. D. 1974. *A Study of the Behaviour of Discontinuous Rock Masses.* Thesis, Ph.D. James Cook University.

HAYASHI, M. 1966. A Mechanism of Stress Distribution in a Fissured Foundation. *Proc. of 1st Congress of ISRM.* **1,** 295–302.

KNOX, W. R. A. 1967. *Fracture Mechanisms in Plain Concrete Subjected to Tension and Compression.* Thesis, Ph.D. Queen's University of Belfast.

KRSMANOVIC, D. & MILIC, S. 1964. Model Experiments on Pressure Distribution in Some Cases of Discontinuum. *Felsmechanik und Ingenieurgeologie* Supp. No. **1,** 72–87.

MAURY, V. 1970. Calcul Theoretiques des Distributions de Constraintes en Milieux Stratifies Discontinus. *Proc. 2nd Congress of ISRM.* **3,** 551–56.

MAURY, V. & HABIB, 1970. Etude sur Models des Distributions de Contraintes on Milieux Stratifies a Frottement. *Proc. 2nd Congress of ISRM.* **3,** 557–62.

MULLER, L. & PACHER, F. 1965. Modellversuche zur Klärung der Bruchgefar geklüfteter Medien, *Felsmechanik und Ingenieurgeologie* Supp II, Springer-Verlag.

NAYLOR, D. J. & PANDE, G. N. 1981. *Finite Elements in Geotechnical Engineering.* Pineridge Press, Swansea.

PECK, R. B. 1976. Rock Foundations for Structures, Rock Engineering for Foundations and Slopes. *ASCE.* **11,** 1–21.

POULOS, H. G. & DAVIS, E. H. 1974. *Elastic Solutions for Soil and Rock Mechanics.* John Wiley and Sons, New York.

REIK, G. & ZACAS, M. 1978. Strength and Deformation Characteristics of Jointed Media in True Triaxial Compression, *Int. Journal of Rock Mechs. and Mining Sci.* **15,** 295–303.

STIMPSON, B. 1970. Modelling Materials for Engineering Rock Mechanics. *Int. Journal of Rock Mechanics and Mining Sci.* **7,** 77–121.

TROLLOPE, D. H. 1968. The Mechanics of Discontinua or Elastic Mechanics. *In*: STAGG, K. G. & ZIENKIEWICZ, O. C. (eds.) *Rock Mechanics in Engineering Practice,* John Wiley, London.

ZACAS, M. 1979. *Behaviour of Rock Masses comprising Rock Structures with Weak inclusions.* Thesis, Ph.D. Paisley College of Technology.

ZIENKIEWICZ, O. C. 1979. *The Finite Element Method in Engineering Science.* McGraw-Hill, London.